20th Australasian Fluid Mechanics Conference
Perth, Australia
5-8 December 2016

The Effect of Target Surface Oscillations on a Turbulent Impinging-Jet Flow

V. Chaugule[1], R. Narayanaswamy[1], A.D. Lucey[1], V. Narayanan[2] and J. Jewkes[3]

[1]Fluid Dynamics Research Group, Department of Mechanical Engineering
Curtin University, Western Australia 6102, Australia

[2]Department of Mechanical and Aerospace Engineering
University of California, Davis, California 95616, USA

[3]Department of Mechanical Engineering
University of South Wales, Pontypridd CF37 1DL, UK

Abstract

The effect of an oscillating target surface on the fluid dynamics of a turbulent impinging jet has been experimentally studied in this paper. The impinging jet effuses from a nozzle with a circular cross-section at a Reynolds number of 5200. The target surface is placed downstream to the nozzle exit at a separation distance of two nozzle diameters, where it oscillates in a direction parallel to the jet impingement direction at a frequency of 20 Hz and at a peak-to-peak displacement amplitude of 0.16 times the nozzle diameter. The flow-field measurements of the mean velocities and the turbulent intensities at 4 displacement positions of the target surface during an oscillation cycle are carried out; two of these positions are considered when the target surface moves away from the jet exit and the other two when it moves towards the jet exit. The measurements at these positions are compared with the corresponding measurements in the impinging-jet flow on a static target surface. The results for the impinging-jet flow on an oscillating target surface show higher mean radial velocities and greater turbulence levels in the wall-jet region, when compared to those in the static target surface.

Introduction

The canonical flow configuration of a jet impinging onto a stationary target surface is extensively used in industry for applications such as drying, heating and cooling of materials. The performance of these applications can be improved in a variety of ways, viz. using an array of jets [3], modifying the geometries of the jet nozzles [2], incorporation of excited [6] and pulsating [1] jets, introduction of swirl in the jet flow [8], and by induced motion of the target surface [4,5,7]. The present paper studies the case of a circular jet of diameter d, impinging on an unheated moving target surface.

The motion of the target surface considered here occurs in a plane parallel to the jet impingement direction, wherein the target surface undergoes an oscillatory motion so that the separation distance between the target surface and the jet exit h oscillates about a mean value. Jet impingement on such an oscillating or vibrating target surface has only been studied sparingly. Wen [7] carried out flow visualizations and heat transfer studies in a swirling jet impingement on a vibrating heated surface. The Reynolds number Re ranged from 440 to 27000 and h varied between $3d$ and $16d$, for surface oscillation frequencies of up to 10.19 Hz and amplitudes of up to 8.1 mm. The variations of the Nusselt number Nu of the vibrating heated surface indicated substantial dependence on the vibrational parameters and Re, showing enhancement of heat transfer with increasing frequency. Ichimiya & Yoshida [4] measured the turbulence intensities in the flow-field and the heat transfer coefficients of the oscillating heated surface in a confined slot impinging jet of width b. The study was carried out for $1000 < \mathrm{Re} < 10000$, $1 < h/b < 4$, and at surface oscillation frequencies of up to 100 Hz and displacement amplitudes of 0.5 mm and 1 mm. The interpretation of the results suggested that at a low value of h/b the area of the jet downstream to the nozzle exit expands in an outward direction and the turbulence intensity increases with increasing frequency of oscillation. The heat transfer estimation showed enhancement at low Re and surface oscillation frequencies at these low values of h/b. Klein & Hetsroni [5] have recently conducted a study on the heat transfer from a vibrating heated silicon chip placed under a confined impinging micro-slot jet. The slot width is 220 μm and Re is between 756 and 1260, while the silicon chip is piezo-electrically vibrated at frequencies up to 400 Hz and at micro-amplitudes up to 150 μm. A maximum increase of 34% in the heat transfer coefficients was observed for the largest Re value, at 246 Hz vibration frequency and at its highest displacement amplitude.

Published works [4,5,7] study the changes in the heat transfer coefficients, but not the changes that occur in the flow-field of the impinging jet, caused by the target surface oscillation. Although some measurements of turbulence intensities are provided [4], detailed analysis of the effect of the target surface oscillations on the impinging-jet flow is not carried out. These studies show that the target surface oscillations contribute to the increase in the heat transfer coefficients of the impinging jet, but what is not completely elucidated is the physical process that causes that change. The impinging-jet flow characteristics are directly affected by the oscillation of the target surface. Therefore, this necessitates the study of the fluid dynamic characteristics of the impinging-jet flow in the presence of the target surface oscillations; which will facilitate better understanding of the convective heat transfer characteristics.

Experiment Methods

Particle image velocimetry (PIV) is used to obtain and compare the mean flow-field velocities and the turbulence intensities of the impinging-jet flow on a static and an oscillating target surface. The jet used is a single submerged air jet, originating from a circular nozzle of exit diameter d = 12.6 mm, at Re = 5200 (based on the jet diameter d). The static target surface is placed at a nozzle-to-surface separation distance of $2d$, downstream of the jet nozzle exit, which is also the mean nozzle-to-surface distance for the oscillating target surface. The target surface undergoes sinusoidal oscillation at a frequency of f_s = 20 Hz and at fixed peak-to-peak displacement amplitude of A_s = $0.16d$. The oscillatory motion of the target surface in the impinging-jet flow is described by the Strouhal number, defined by $St = f_s A_s / U_b$. For the values of the target surface oscillation parameters and the bulk jet-flow speed of U_b = 6.21 m/s, the Strouhal number is St = 0.0065.

A schematic of the experimental set-up used is shown in figure 1. Clean air flow and a flow seeded with atomized olive oil particles are fed via a Y-hydraulic fitting into a straight circular jet pipe. Both the clean air flow and the seeded flow are metered before they enter the jet pipe. The circular jet pipe is a polyvinyl chloride (PVC) pipe of length 0.5 m, with a copper reducer coupling (2:1 contraction) attached to its end that forms the jet nozzle. The jet nozzle exit has an inner diameter of d = 12.6 mm. A flow straightener is installed in the entrance of the pipe to eliminate any swirl generated by the Y-hydraulic fitting.

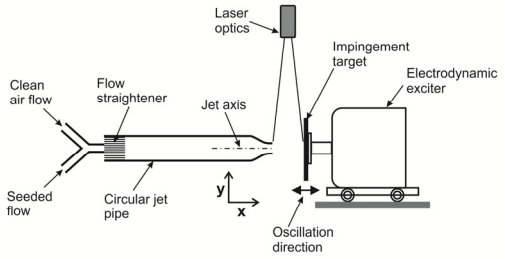

Figure 1. Schematic of the experimental set-up.

The impingement target surface is a 0.5 mm thick, square aluminium sheet of side measuring 150 mm. A 3 mm thick medium-density fibreboard (MDF), having the same area as the aluminium sheet, is attached to the underside of the aluminium sheet. The surface of the aluminium sheet facing the jet is painted with a black enamel to reduce reflections caused by the laser light. The MDF plate is fixed to the mount of an electrodynamic exciter, which sits on top of a platform with wheels; this arrangement allows setting a required value of the mean nozzle-to-surface separation distance. Sinusoidal input signal to the electrodynamic exciter is provided via a function generator. The frequency of surface oscillation and its displacement amplitude are measured using a single axis accelerometer, attached to the impingement surface, whose conditioned output is read on a digital oscilloscope. The output settings of the function generator are then adjusted to achieve the required oscillation frequency and amplitude of the target surface.

A time-resolved 2D-PIV system (Dantec Dynamics) is used in this study. Single-exposure double-frame images of the flow-field are captured using a PIV camera (Phantom M-310) with a pulse delay of 21 µs. The camera objective is an AF Micro-Nikkor lens (f = 200 mm) whose exposure is set at f/8 with a magnification of 0.4. The x-axis in the PIV image frame is parallel to the jet axis while the y-axis is perpendicular to the jet axis as shown in figure 1. The PIV measurement area covers only one-half of the illuminated flow regions (as the flow is axisymmetric), with a field-of-view of approximately $5d \times 3d$ ($x \times y$). The frequency of acquisition for the jet impingement on a static target surface is set at 50 Hz, whereas to extract the impinging jet flow-field information at transient positions of the target surface in an oscillation cycle, the acquisition frequency for the jet impingement on an oscillating target surface is set at 200 Hz. The time between successive image-pairs in these acquisitions ensure that the image pairs are statistically time independent. In order to evaluate the flow field at different positions (phases) of the target surface in the jet impingement on an oscillating target surface, 1000 image pairs were extracted corresponding to a given position of the target surface in an oscillation cycle. An equal number of image pairs are also acquired for the jet impingement on a static target surface.

The acquired images are analyzed using software (DynamicStudio) that accompanies the PIV system. The velocity vectors are calculated over an interrogation area of 16 × 16 pixels (50% overlap) using a multi-pass multi-grid cross-correlation analysis recipe with deforming windows and sub-pixel refinement modules. The resulting velocity vector maps are then scanned for any outliers and the rejected vectors (if any) are substituted by a median vector. The maximum particle displacement was determined to be less than 3 pixels, and the spatial resolution between the resulting velocity vectors is 0.031D, i.e. approximately 0.4 mm.

The target surface oscillates about a mean nozzle-to-surface separation distance of 2d, such that nozzle-to-surface separation distance varies between 1.92d and 2.08d. The flow characteristics in the jet impingement on an oscillating target surface have been measured and analyzed at 4 positions (phases) of the target surface in an oscillation cycle. Two of these positions (A1 and A2) are when the target surface is moving away from the jet exit, while the other two (T1 and T2) are when the surface is moving towards the jet exit.

Results and Discussion

The flow directions along the x and y axis are considered as the axial and radial flow directions respectively. The results presented are the measurements of the mean velocity components and the rms velocity fluctuation components for the jet impingement on a static target surface (hereafter referred to as STS) and for the jet impingement on an oscillating target surface (hereafter referred to as OTS). In all of the results, the dimensions along the axes have been scaled with respect to the jet nozzle exit diameter d. The dimensionless axial coordinate is expressed as $x^+ = x/d$, with $x^+ = 0$ at the target surface, and the dimensionless radial coordinate as $y^+ = y/d$, with $y^+ = 0$ at the jet axis. For all results, the mean axial and radial velocity components, and the rms axial and radial velocity fluctuation components have been scaled with respect to the mean-centerline jet exit velocity ($\langle u_{cj} \rangle$). These are denoted respectively by $u^+ = \langle u \rangle / \langle u_{cj} \rangle$, $v^+ = \langle v \rangle / \langle u_{cj} \rangle$, $u'^+ = \sqrt{\langle u'^2 \rangle} / \langle u_{cj} \rangle$, and $v'^+ = \sqrt{\langle v'^2 \rangle} / \langle u_{cj} \rangle$.

Static Target Surface (STS) jet impingement

The mean axial and radial velocity contour plots are shown in figure 2(a) and 2(b) respectively. In figure 2(a), the length of the potential core region, wherein the jet retains most of its maximum mean axial velocity, is observed to extend up to a distance of 0.7d above the target surface (1.3d from the jet exit). The mean axial velocity reduces as the jet approaches closer to the target surface, and upon impingement the jet deflects in a radial direction to form a wall-jet. In figure 2(b), the maximum mean radial velocity magnitude of $v^+ = 0.75$ occurs at a radial location $y^+ = 0.8$. The wall-jet advances beyond this radial location with decreasing mean radial velocity and increasing thickness in the wall-normal x^+ direction.

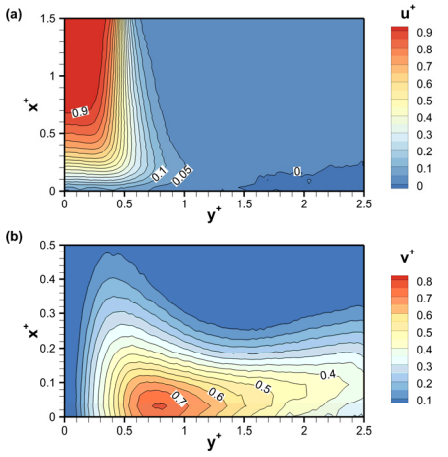

Figure 2. STS contours (a) mean axial velocity (b) mean radial velocity

The rms axial and radial velocity fluctuations are shown in figure 3(a) and figure 3(b) respectively. In figure 3(a), the fluctuation in the free-shear layer reaches a maximum magnitude of $u'^{+} = 0.19$, while that in the wall-jet does not exceed a value of $u'^{+} = 0.12$, with the maximum occurring in the vicinity of the radial location $y^{+} = 2$. The near-wall fluctuations are closer to a magnitude of $u'^{+} = 0.08$. In figure 3(a) the contour levels between $u'^{+} = 0.13$ and 0.16 have not been shown for clarity. As the wall-jet advances radially, it is increasingly affected by the shear from the wall as well as from the top mixing layer. This decelerates the wall-jet and increases its turbulence levels as observed in figure 3(b). The maximum rms radial velocity fluctuation in the wall-jet region is $v'^{+} = 0.19$, which occurs just beyond the radial location $y^{+} = 1.5$.

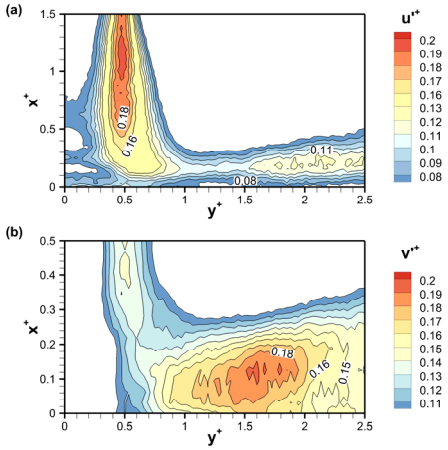

Figure 3. STS contours (a) rms axial velocity fluctuation (b) rms radial velocity fluctuation

Oscillating Target Surface (OTS) jet impingement

The contours of the mean axial velocity of the jet at the 4 target surface positions in an oscillation cycle are shown in figure 4. The origin of the non-dimensional axial coordinate $x^{+} = 0$ is at the wall location of the oscillating target surface at each of its displacement positions. The displacement of each of these positions, compared to the position of the static target surface (mean nozzle-to-surface separation position), is illustrated on top of the corresponding contours. The vertical dashed lines represents the position of the static target surface, while the solid vertical lines represents the position of the target surface at the corresponding phase in an oscillation cycle, with the arrows pointing towards the jet exit.

In figure 4 at position A1, the mean axial velocities are higher than those observed in the static target surface (STS - figure 2(a)). At position A2, the mean axial velocities in the impingement region are similar to those in STS, but higher in the wall-jet region of $y^{+} > 1.5$. The length of the potential regions in A1 and A2 are only marginally longer than that in STS. These changes occur because the target surface moves increasingly away from the jet exit, and in the positive direction of the axial velocity, as the displacement position changes from A1 to A2, which increases the axial velocity of the jet and also of the ambient fluid, relative to the target surface. At positions T1 and T2, the mean axial velocity variations are similar to those in STS, except in the region $1 < y^{+} < 1.5$, where the axial velocity magnitudes are observed to be lower than those in STS. This is because the direction of motion of the target surface is opposite to the axial velocity direction of the jet, which causes a reduction in the relative axial velocity of the jet. The target surface moves towards the jet exit as it progresses from position T1 to T2. The primary cause for the above mentioned observations is the high acceleration magnitudes of the target surface at each of those displacement positions, rather than the peak velocity of the oscillating surface relative to the axial velocity of the jet, which is only about 2% of U_b.

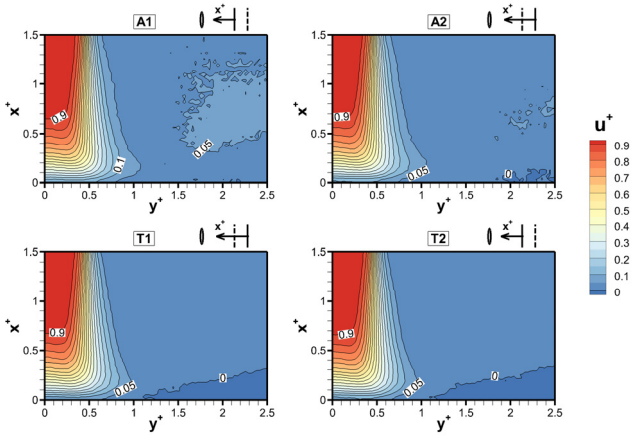

Figure 4. OTS – mean axial velocity contours at the target surface positions.

The mean radial velocity contours in the wall-jet are shown in figure 5. At all the positions A1, A2, T1 and T2, the mean radial velocities and the radial extent of the acceleration region are higher than those in STS (figure 2(b)), with position A1 having lower corresponding values than other positions. The oscillatory motion of the target surface does not directly affect the mean radial velocity in the wall-jet, because the direction of the target surface oscillation is perpendicular to the radial velocity direction. The reasons for the above mentioned variations in the mean radial velocities in OTS, when compared to that in STS, lie in their relationship with the mean axial velocities through the continuity equation. As observed in figure 4, the oscillatory motion of the target surface directly affects the mean axial velocities. Therefore, in order to satisfy conservation laws, at positions where lower values of the gradient of the mean axial velocity (along the axial direction) exist, the corresponding values of the mean radial velocities are higher. It should be noted that at positions A1 and T2, when the oscillating target surface is closer to the jet exit than the static target surface, the value of x^{+} is actually lower from that at the static target surface.

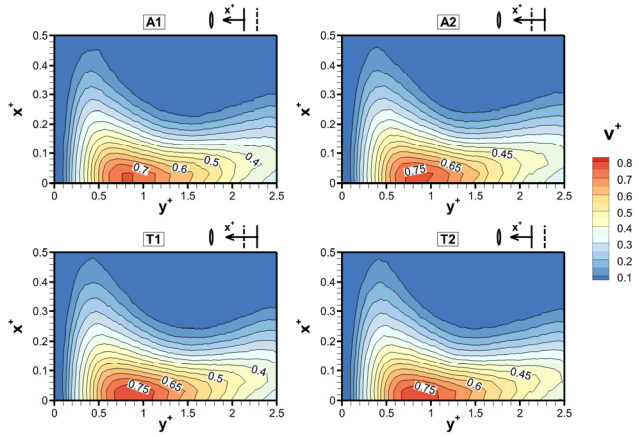

Figure 5. OTS – mean radial velocity contours at the target surface positions.

The rms axial velocity fluctuation at the target surface positions are shown in figure 6. At position A1, the axial velocity fluctuations in the wall-jet region are higher than those in STS (figure 3(a)), while at positions A1 and A2 the fluctuations in the free-shear layer of the jet are lower than those in STS. At positions T1 and T2, the axial turbulence in the free-shear layer of the jet and in the wall-jet has magnitudes similar to those in STS. These changes in the rms axial velocity fluctuation are

caused by the effect of the motion of the target surface on the axial velocity of both the jet and the ambient fluid. As the target surface moves away from the jet exit, it increases the axial velocity of the jet as well as of the ambient fluid which results in lower shear in the free mixing layer, and larger fluctuations in the slower moving wall-jet due to higher entrainment. As the velocity of the oscillating target surface is very low in comparison to the axial bulk speed of the jet, the motion of the target surface towards the jet exit does not affect the impinging-jet flow to such an extent as to alter its axial turbulence intensities.

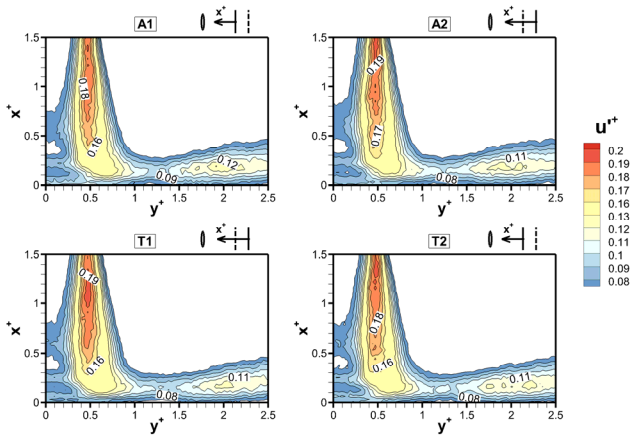

Figure 6. OTS – rms axial velocity fluctuation contours at the target surface positions.

The rms radial velocity fluctuation contours for the target surface positions are shown in figure 7. The radial turbulence levels in the wall-jet at positions A1 and T2 are significantly higher than those in STS (figure 3(b)). While at positions A2 and T1 the rms radial velocity fluctuations in the wall-jet are slightly lower than that in STS. These opposing trends in the radial turbulence intensities are due to the increased entrainment in the wall-jet at position A1 and higher mean radial velocities in the wall jet at position T2. These positions also coincide with the position of the target surface closest to the jet exit. It is interesting to note that at all the positions, the near-wall fluctuations in the vicinity of the radial location $y^+ = 2$ are higher than those in STS. These patterns occur because of the effect of high acceleration of the target

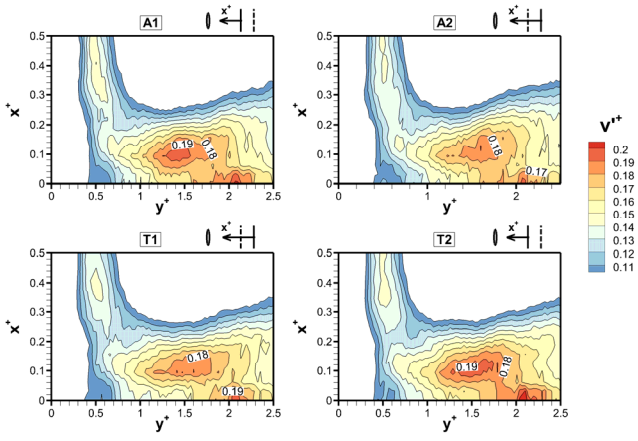

Figure 7. OTS – rms radial velocity fluctuation contours at the target surface positions.

surface on the wall-jet flow at these displacement positions. The effect of the oscillating target surface in increasing the radial turbulence levels from that observed in the static target surface, is larger in those radial locations where the presence of the jet diminishes.

Conclusions

The effect of target surface oscillation on the fluid dynamic characteristics of a turbulent impinging jet has been experimentally studied in this paper. The impinging-jet flow characteristics are significantly altered due to the oscillatory motion of the target surface. These changes are observed in both the wall-jet and the free-jet regions, as well as in the ambient fluid region. The oscillatory motion of the target surface increases the mean radial velocities in the wall-jet and also generates higher turbulence levels in the mixing layer in the wall-jet, when compared to those present in the jet impingement on the static target surface. These higher turbulent intensities are probable causes for enhanced convective heat transfer observed in the impinging-jet flow on an oscillating target surface.

Acknowledgments

The authors gratefully acknowledge the support from the Australian Research Council (ARC) Discovery Project Grant - DP 130103271.

References

[1] Alimohammadi, S., Murray, D.B. & Persoons, T., On the Numerical–Experimental Analysis and Scaling of Convective Heat Transfer to Pulsating Impinging Jets, *Int. J. Therm. Sci.*, **98**, 2015, 296-311.

[2] Dano, B.P., Liburdy, J.A. & Kanokjaruvijit, K., Flow Characteristics and Heat Transfer Performances of a Semi-Confined Impinging Array of Jets: Effect of Nozzle Geometry, *Int. J. Heat Mass Trans.*, **48(3)**, 2005, 691-701.

[3] Geers, L.F., Tummers, M.J. & Hanjalić, K., Experimental Investigation of Impinging Jet Arrays, *Exp. Fluids*, **36(6)**, 2004, 946-958.

[4] Ichimiya, K. & Yoshida, Y., Oscillation Effect of Impingement Surface on Two-Dimensional Impingement Heat Transfer, *J. Heat Transfer*, **131**, 2009, 011701-1-6.

[5] Klein, D. & Hetsroni, G., Enhancement of Heat Transfer Coefficients by Actuation Against an Impinging Jet, *Int. J. Heat Mass Trans.*, **55**, 2012, 4183-4194.

[6] Roux, S., Fénot, M., Lalizel, G., Brizzi, L.E. & Dorignac, E., Experimental Investigation of the Flow and Heat Transfer of an Impinging Jet Under Acoustic Excitation, *Int. J. Heat Mass Trans.*, **54(15)**, 2011, 3277-3290.

[7] Wen M-Y, Flow Structures and Heat Transfer of Swirling Jet Impinging on a Flat Surface with Micro-Vibrations, *Int. J. Heat Mass Trans.*, **48**, 2005, 545-5.

[8] Yang, H.Q., Kim, T., Lu, T.J. & Ichimiya, K., Flow Structure, Wall Pressure and Heat Transfer Characteristics of Impinging Annular Jet with/without Steady Swirling, *Int. J. Heat Mass Trans.*, **53(19)**, 2010, 4092-4100.